Journal of Fluorescence, Vol. 13, No. 6, November 2003 (©2003)

Dipolar Relaxation Times of Tryptophan and Tyrosine in Glycerol and in Proteins: A Direct Evaluation from Their Fluorescence Decays

Giampiero Mei,[1,2] Almerinda Di Venere,[1,2] Alessandro Finazzi Agrò,[1] Fabio De Matteis,[2,3] and Nicola Rosato[1,2,4]

Received August 12, 2003; revised September 16, 2003; accepted September 16, 2003

The dipolar relaxation process induced around tryptophan, indole and tyrosine in viscous media, as well as in several single tryptophan-containing proteins (staphylococcal nuclease, ribonuclease T1, melittin and albumin), has been studied by dynamic fluorescence measurements. A new theoretical model has been developed, including the relaxation dynamics directly in the fluorescence decay function. The phase shift and demodulation data have been fitted with this new algorithm which allows to resolve the different relaxation times influencing the fluorophore excited state. These parameters are in a good agreement with those measured with the traditional time-resolved emission spectroscopy. The results indicate that indeed a correlation exists between the radiative rate change obtained with the new model and the temporal spectral shift reported in the literature. Finally, this new approach has also been extended to the case of superoxide dismutase and phosphofructokinase, allowing to measure the relaxation time even in proteins lacking a temporal spectral shift during the fluorphore's lifetime.

KEY WORDS: Dipolar relaxation; tryptophan; time resolved fluorescence.

INTRODUCTION

Tryptophan fluorescence is extremely sensitive to the surrounding microenvironment. Such peculiar feature makes this intrinsic chromophore of proteins a very suitable probe to investigate both structural fluctuations and conformational changes of these macromolecules in solution [1]. Tyrosine fluorescence is also widely used in protein spectroscopy, especially in the absence of tryptophan residues [2]. Generally protein fluorescence is characterized by a complex, multi-exponential function or by a continuous distribution of lifetimes. This heterogeneity has been ascribed to the different environments provided by the protein matrix around its intrinsic chromophores. Complex fluorescence decays in single-tryptophan containing proteins might have at least two possible explanations: static heterogeneity, due to different ground state conformations and dynamics processes that affect the excited state of the aromatic ring. An ideal experiment that allows to distinguish static heterogeneity from dynamic heterogeneity would be the recording of the fluorescence decay of one single macromolecule. Although a few measurements of this kind have been reported in literature [3], at present the recording of the intrinsic fluorescence decay from a single protein is difficult to achieve due to photobleaching effects. If in the future such experiments will

[1] Department of Experimental Medicine and Biochemical Sciences, University of Rome "Tor Vergata," Via Montpellier, 1, 00133 Rome, Italy.
[2] INFM, Genova, Italy.
[3] Department of Physics, University of Rome "Tor Vergata," Rome, Italy.
[4] To whom correspondence should be addressed; e-mail: nicola.rosato@uniroma2.it.

ABBREVIATIONS: NATA, *N*-acetyl-*L*-tryptophanamide; TRES, time-resolved emission spectroscopy; HSA, human serum albumin; RNAase-T1, ribonuclease T1; PFK, phosphofructokinase; HSOD, human superoxide dismutase.

1053-0509/03/1100-0467/0

reveal that even the fluorescence decay of a single protein is heterogeneous, new fitting models will be required. These models will have to take into account the conformational dipolar re-arrangements around the excited fluorophore during its lifetime. This relaxation process is indeed assumed to be induced by the fast increase of the probe dipolar moment upon excitation from the ground to the excite state [4].

Similar events generally produce a time dependent red-shift of the fluorescence spectrum (known as spectral relaxation) and an increase of the fluorescence lifetime at longer emission wavelengths [1]. Both steady state and dynamic fluorescence parameters are expected to be influenced by dipolar relaxation [5–7]. The detection of such phenomena is obviously dependent on the time-course of the relaxation process. While aqueous buffers relaxation is usually fast (tens of picoseconds or less), re-orientation of protein polar residues spatially close to the emitting species is expected to occur in the same range of proteins' intrinsic fluorescence lifetime, i.e. from sub-nanoseconds to nanoseconds [8]. This condition is usually satisfied for fluorophores in viscous solvent [1], micelles [9], liposomes [10–11] and membranes [12]. In these systems the decay rate may be, therefore affected by relaxation processes. A complex fluorescence decay may be also displayed by single tryptophan (or tyrosine-) containing proteins in "single molecule" experiments, since the relaxation could produce a modification of the emission photon probability from the excited state of the fluorescence probe.

In a previous paper [13] we have proposed to fit the fluorescence decay of single tryptophan proteins with a new mathematical model intrinsically containing the dipolar relaxation effect of the aminoacidic residues surrounding the excited fluorophore. Despite the probability λ of spontaneous emission was assumed to be time-dependent, no distinction was made between the radiative K_F and no radiative K_N decay rates.

In this study we have extended the model to the general case of independently time-dependent K_F and K_N functions. The new model has been tested on experimental data and the results compared (when possible) with those obtained with the traditional methodologies used to study the spectral relaxation effects.

EXPERIMENTAL SECTION

Materials

Indole (99+%), spectrophotometric grade glycerol and propylene glycol were purchased from Aldrich, Merk and Fluka, respectively.

N-acetyl-L-tryptophanamide (NATA), L-tyrosine, human serum albumin (HSA), honey bee venom melittin, ribonuclease T1 (RNAase-T1 from *aspergillus oryzae*) and phosphofructokinase from *bacillus stearothermophilus* (PFK) were purchased from Sigma.

Human superoxide dismutase (HSOD) was purified from human erythrocytes [14]. Staphylococcal nuclease was a generous gift from Dr. Gianfranco Gilardi (Imperial College, London).

Methods

Dynamic fluorescence measurements were performed at the Laboratorio di Spettroscopia ai Picosecondi, LASP (University of Rome, "Tor Vergata," Italy) using the phase-shift and demodulation technique. The excitation source was the harmonic content of a mode-locked Nd-Yag laser as previously described [15], or a frequency-modulated xenon arc lamp. The excitation was polarized at the "magic angle" to eliminate rotational effects on the fluorescence lifetime measurements (1).

The data were analyzed by minimizing the reduced chi-squared value with routines based on the Marquardt algorithm [16].

THEORY OF DECAY ANALYSIS

Ensemble of Identical Fluorophores in a Homogeneous and Static Environment

In this trivial case the fluorescence decay is a well known monoexponential function [1]. In fact, indicating with $n(t)$ the number of molecules still excited at time t, and with $\lambda = K_F + K_N$ the global (radiative plus non radiative) emission probability per unit time, the following equations hold:

$$dn(t) = -\lambda n(t)\, dt$$

$$\ln \frac{n(t)}{n_0} = -\int \lambda dt$$

$$n(t) = n_0 e^{-\int \lambda dt}$$

where $n_0 = n(0)$ is the number of excited molecules at $t = 0$.

If λ is assumed to be time-independent, i.e. $\lambda = \text{const}$:

$$n(t) = n_0 e^{-\lambda t} \tag{1}$$

and the lifetime of the excited state is $\tau = 1/\lambda$.

Since the measured fluorescence intensity is proportional to the population of the excited molecules through

K_F, the fluorescence decay, $f(t)$, is given by:

$$f(t) = K_F n(t) = K_F n_0 e^{-\lambda t} = f_0 e^{-\lambda t} \qquad (2)$$

f_0 being the fluorescence intensity at time $t = 0$.

Single Molecule in a Homogeneous and Static Environment

For a single molecule excited at time $t = 0$ it is possible to obtain an expression similar to Eq. (1). Indicating with $\gamma(t)$ the probability at time t that the molecule is still excited and with $\delta(t)$ the probability that the molecule has reached the ground state:

$$\gamma(t) + \delta(t) = 1$$

If λ is the de-excitation probability per unit time of the single molecule, the decay probability in the time interval $(t \div t + dt)$ is:

$$\delta(t + dt) - \delta(t) = \gamma(t)\lambda dt = d\delta$$

i.e. λdt multiplied by the probability that the molecule is still excited. Since $d\delta = -d\gamma$, it follows that:

$$-d\gamma = \gamma(t)\lambda dt$$

and

$$\gamma(t) = \gamma_0 e^{-\lambda t} = e^{-\lambda t} \qquad (3)$$

where $\gamma_0 = \gamma(0) = 1$ since the molecule is excited at the initial time.

As for Eq. (2), the probability of emitting one photon at time t is:

$$f(t) = K_F \gamma(t) = K_F e^{-\lambda t}$$

For a single molecule the total fluorescence decay is obviously obtained repeating the excitation and collecting each time the single emitted photon. Thus, the histogram of the arrival times is built up *a posteriori*.

Single Molecule in a Homogeneous Environment in Presence of a Time-Dependent Dipolar Relaxation

In this case the probability of de-excitation, λ, is not constant as it value changes during the lifetime of the excited state. This effect is due to the relaxation process that modifies the number and the efficiency of the collisions with the surrounding dipoles. As a consequence Eq. (3) has the following more general form:

$$\gamma(t) = e^{-\int_0^t \lambda(\vartheta) d\vartheta} \qquad (4)$$

Thus, an explicit expression for $\lambda(t)$ is required to fit the experimental data.

Since, at present, a quantum mechanical model is not available to predict an analytical expression for $\lambda(t)$, we have attempted to fit the data assuming an exponential decay function:

$$\lambda(t) = \lambda_\infty + (\lambda_0 - \lambda_\infty) e^{-\frac{t}{\tau_R}} \qquad (5)$$

In this case $\lambda_0 = \lambda(0)$ is the decay probability at time $t = 0$ (i.e. immediately after excitation and before dipolar relaxation) and λ_∞ is the decay probability at times much longer than the relaxation time, τ_R. Equation (5) is very simple to use as it depends only on three free parameters (λ_0,λ_∞ and τ_R). The integration of Eq. (4) with $\lambda(t)$ given by Eq. (5) yields:

$$\gamma(t) = e^{-\tau_R(\lambda_0 - \lambda_\infty)} e^{-\lambda_\infty t} e^{\tau_R(\lambda_0 - \lambda_\infty) e^{-\frac{t}{\tau_R}}} \qquad (6)$$

and for the fluorescence decay:

$$f(t) = K_F \gamma(t) \qquad (7)$$

Given a single molecule experiment, the fit of the experimental data (in presence of relaxation) using Eq. (7) allows to directly obtain $\tau_0 = \frac{1}{\lambda_0}$ (i.e. the lifetime immediately after excitation), $\tau_\infty = \frac{1}{\lambda_\infty}$ (i.e. the lifetime at the very end of the relaxation process) and the average time of the relaxation, τ_R.

Equation (7) is valid only as long as K_F does not change with time. However, it is well known that during dipolar relaxation a red shift of the emission spectrum may occur [1,8]. Therefore, in the more general case, a time–dependent probability for both the decay rate, $K_F = K_F(t)$, and the non radiative processes, $K_N = K_N(t)$, must be taken into account. Since spectral relaxation generally occurs following a single or double exponential function [1,8], we have assumed:

$$K_F(t) = K_F^\infty + (K_F^0 - K_F^\infty) e^{-\frac{t}{\tau_F}}$$

and

$$K_N(t) = K_N^\infty + (K_N^0 - K_N^\infty) e^{-\frac{t}{\tau_N}} \qquad (8)$$

and, since $\lambda(t) = K_F(t) + K_N(t)$, the total fluorescence decay can be written as:

$$f(t) = K_F(t) e^{-\int_0^t [K_F(\vartheta) + K_N(\vartheta)] d\vartheta} \qquad (9)$$

This equation, which contains 6 free parameters (K_F^0, K_N^0, K_F^∞, K_N^∞, τ_F, τ_N), allows to obtain the radiative, τ_F, and non-radiative, τ_N, relaxation times directly from the fluorescence decay, without any measurements of the spectral red-shift during the relaxation process. If the two events (spectral and lifetime relaxation) are characterized by a similar time-scale (i.e. $\tau_F \approx \tau_N$), then Eq. (9) depends only on 5 free parameters.

It is worth mentioning that 5 free parameters are also required in other commonly used fluorescence decay models, namely a triple discrete exponential function and a double lorentzian/gaussian continuous distribution of lifetimes [17–19].

Ensemble of Identical Molecules in a Homogeneous Environment in Presence of a Time-Dependent Dipolar Relaxation

Equation (9), which has been obtained for a single molecule, may be extended to the case of an ensemble of identical molecules, simultaneously excited at time $t = 0$. In fact, assuming that the relaxation process occurs in the same way for all molecules:

$$f(t) = f_0 K_F(t) e^{-\int_0^t [K_F(\vartheta)+K_N(\vartheta)]d\vartheta} \qquad (10)$$

where f_0 is the fluorescence intensity at time $t = 0$.

Equation (10) has been used in the present study to fit the experimental dynamic fluorescence data of tryptophan, tyrosine and single tryptophan-containing proteins.

RESULTS AND DISCUSSION

In order to test whether the new mathematical model can be used to fit experimental fluorescence decays, we have performed several dynamic fluorescence experiments on aromatic fluorophores (indole and tyrosine) and on selected proteins, which are known to relax in the nanosecond time-scale. Furthermore, a couple of single-fluorophore proteins (whose relaxation has not yet been demonstrated by traditional methods) have been taken into account and their dynamic fluorescence has been interpreted in terms of both single and double relaxation process.

N-acetyltryptophanamide, Indole and Tyrosine

It is well known that tryptophan in water exhibits a double exponential decay which has been ascribed to the presence of rotational isomers (rotamers) characterized by different distances between the indole ring and the charged amino group [20–23]. This intrinsic complexity of the tryptophan zwitterionic form is instead absent in the indole decay and in the dynamic fluorescence of some analogues such as NATA, a tryptophan neutral derivative, which is structurally closer to tryptophan residues in proteins [24]. Both time- and frequency-domain techniques have in fact demonstrated that indole and NATA in aqueous solution display a single fluorescence lifetime around 4.8 and 3.0 ns, respectively [24]. These values are of course too long with respect to solvent molecules diffusion, making impossible any detection of indole and NATA dielectric relaxation in aqueous buffer, at room temperature. On the other hand the lifetime of NATA in propylene glycol exhibits a strong dependence on the emission wavelength [25], suggesting that dipolar relaxation around the excited indole might become detectable in a more viscous solvent. We have measured the fluorescence decay of NATA in glycerol at 15°C and the results are reported in Fig. 1. Panel a and panel b represent the five free parameters used in two different fitting functions: a classical triple discrete exponential decay and the single relaxation function (i.e. $\tau_F = \tau_N$) described by Eq. (10). In this last case the relaxation process resulted to be characterized by a $\tau_R \approx 1.1$ ns. No statistical improvement in the fit (i.e. chi-squared value and residuals distribution) was obtained using two distinct relaxation times, i.e. separating the contribution of $K_N(t)$ and $K_F(t)$ to the fluorescence decay (with $\tau_F \neq \tau_N$).

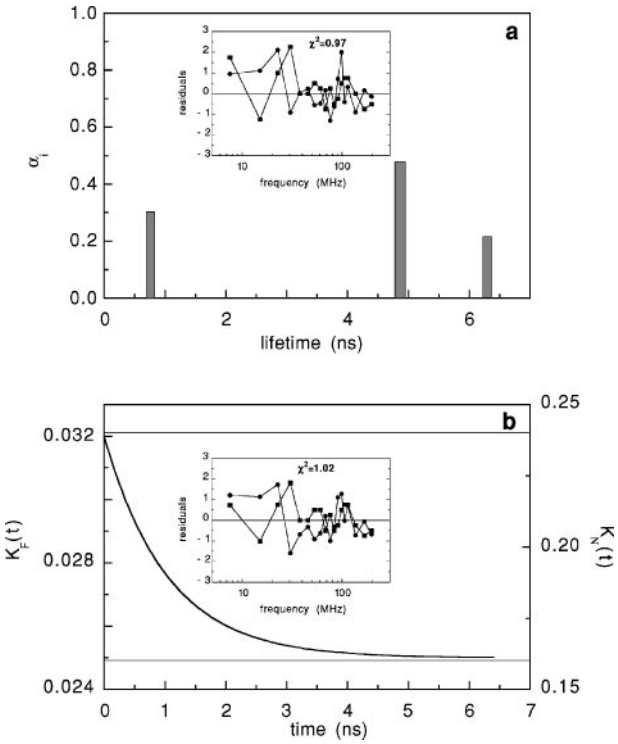

Fig. 1. Fluorescence decay parameters and weighted residuals pattern for NATA in glycerol at 15°C. Panel a: discrete fluorescence lifetimes obtained fitting phase and modulation data with a triple exponential decay function. Panel b: best fit obtained with a single relaxation time function (i.e. $\tau_F = \tau_N = \tau$) according to Eq. (10) (with $K_F^0 = 0.032 \pm 0.003$ ns^{-1}; $K_F^\infty = 0.025 \pm 0.003$ ns^{-1}; $K_N^0 = 0.24 \pm 0.01$ ns^{-1}; $K_N^\infty = 0.16 \pm 0.01$ ns^{-1}; $\tau_R = 1.0 \pm 0.1$ ns). In the insets the reduced chi-squared value is reported for each fit.

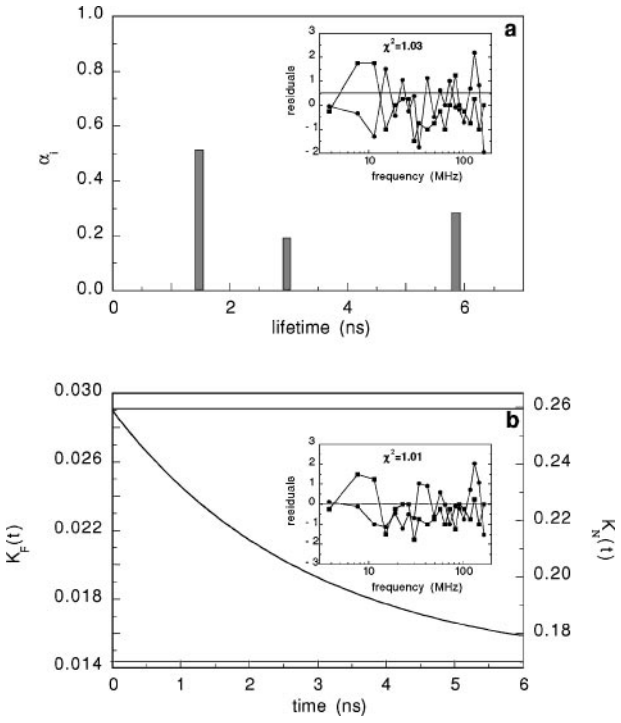

Fig. 2. Fluorescence decay parameters (see the legend of Fig. 1 for details) for indole in propylene glycol at 8°C. Panel a: triple exponential decay function parameters. Panel b (single relaxation function): $K_F^0 = 0.029 \pm 0.003$ ns^{-1}; $K_F^\infty = 0.014 \pm 0.003$ ns^{-1}; $K_N^0 = 0.26 \pm 0.01$ ns^{-1}; $K_N^\infty = 0.17 \pm 0.01$ ns^{-1}; $\tau_R = 2.9 \pm 0.2$ ns).

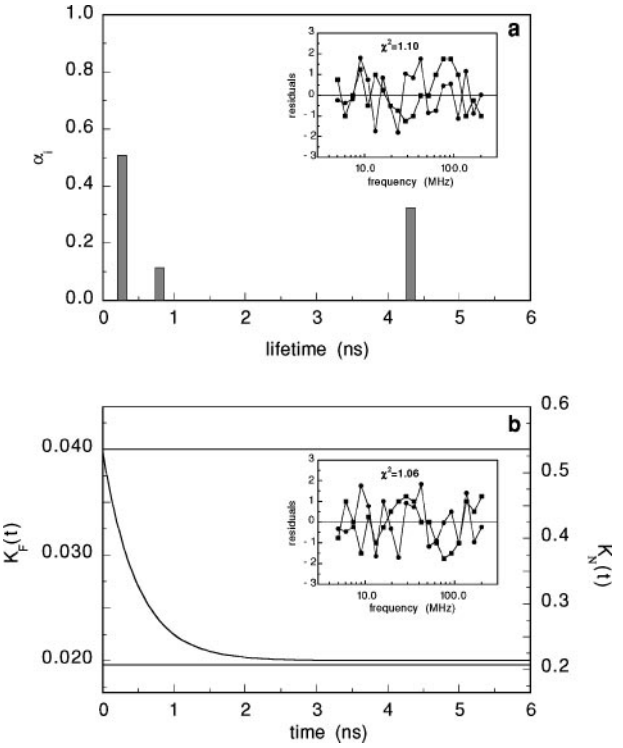

Fig. 3. Fluorescence decay parameters (see the legend of Fig. 1 for details) for tyrosine in glycerol at 10°C. Panel a: triple exponential decay function parameters. Panel b (single relaxation function): $K_F^0 = 0.040 \pm 0.004$ ns^{-1}; $K_F^\infty = 0.020 \pm 0.003$ ns^{-1}; $K_N^0 = 0.53 \pm 0.02$ ns^{-1}; $K_N^\infty = 0.21 \pm 0.02$ ns^{-1}; $\tau_R^F = 0.48 \pm 0.03$ ns).

The emission of indole in a viscous solvent is also known to be affected by dielectric relaxation [26–28]. The fluorescence decay of indole in propylene glycol also requires at least three discrete exponentials to satisfactorily fit the data (Fig. 2a). On the other hand, using Eq. (10) a relaxation time of 3.1 ns was obtained (Fig. 2b), in good agreement with the value previously recovered with the traditional time-resolved emission spectroscopy (TRES) methodology (i.e. 2.8 ns) [27]. Also in this case a single relaxation time was sufficient to fit the data.

Unlike tryptophan, tyrosine emission is insensitive to solvent polarity: its emission occurs between 303 and 305 nm in water as well as in proteins and polypeptides [2]. Furthermore, the dipole moment of phenol is not particularly high both in the ground and in the excited state [29] making almost impossible to detect any relaxation process by traditional methods (i.e. TRES, edge excitation spectroscopy etc. . .). Since intrinsically-contained relaxation in the fluorescence decay may be instead taken into account using Eq. (10), we performed dynamic fluorescence experiments on tyrosine under different experimental condition.

Tyrosine in water is known to be characterized by a single fluorescence lifetime [2]. In a control measurement we have obtained $\tau = 3.33$ ns ($\chi^2 = 1.07$) in good agreement with the average lifetime reported in literature (≈3.4 ns). A considerable deviation from a monoexponential decay has been instead obtained increasing the viscosity by addition of glycerol. In particular at least three exponential had to be included in the fitting function in order to get a reasonable chi-squared value and a random distribution of weighted residuals (Fig. 3a and inset). The analysis of phase and demodulation data by a single and a double relaxation function suggest that one relaxation time is sufficient to fit the experimental points (Fig. 3b). Interestingly, a much faster relaxation rate seems to characterize tyrosine emission (0.48 ns) with respect to tryptophan in the same condition (1.1 ns, Fig. 1).

For the three examples examined, it is worth mentioning that the discrete exponential function and the relaxation model yield the same reduced chi-squared value and similar residuals pattern, randomly distributed around zero, according to a gaussian statistic. Actually, the physical meaning of a triple exponential decay is not so clear

for both tryptophan and tyrosine. In principle, the longer components could be assigned to the fully relaxed fluorophores, while shorter lifetimes would represent the emission of non-relaxed and partially relaxed states. However, this interpretation does not give any direct information on the relaxation process that involves the fluorophore excited state(s). On the other hand, the results reported in Fig. 1, 2 and 3 demonstrate that the relaxation time is intrinsically contained in the fluorescence decay of both tryptophan and tyrosine. Thus, in the case of viscous solvent, the relaxation process represented by Eq. (10) is sufficient to explain the deviation from the single lifetime decay that instead characterizes the emission of these fluorophores in aqueous buffers.

Single Tryptophan-Containing Proteins Which Exhibit Spectral Relaxation

Unlike tryptophan in aqueous buffers, the lifetime of several single-tryptophan proteins is strongly dependent on the emission wavelength, even at room temperature [25]. In several cases, their steady-state fluorescence spectrum has been also found to depend on the excitation wavelength [30]. These findings have been interpreted in terms of slow dipolar relaxation processes which take place in the nanosecond time scale and which involve the reorientation of groups surrounding the tryptophan residue [30]. According to this model, the protein matrix behaves as a viscous medium, slowing down the relaxation approximately to the same time-range of fluorescence emission. In several cases this hypothesis has been confirmed by TRES experiments, measuring the time-dependent fluorescence spectral shift. This effect is particularly evident in proteins emitting at intermediate wavelength values (325–341 nm) [30,31]. Taking advantage of the results reported in literature, we have performed dynamic fluorescence on a few single-tryptophan proteins, namely staphylococcal nuclease, RNAase T1, melittin and human serum albumin.

Staphylococcal nuclease is a small globular protein (≈17 kDa) whose fluorescence spectrum is centered around 341 nm. Its emission decay in aqueous buffer is characterized by two or three different components ($\tau_1 \leq 1$ ns; $\tau_2 \approx 2$–4 ns; $\tau_3 \approx 5$–6 ns), as shown by both frequency- and time-domain techniques [32,33]. The dynamic fluorescence of staphylococcal nuclease in viscous solvents is known to be strongly dependent on temperature and spectral relaxation has been proved to occur in the nanosecond time range [34]. In principle, the phase and demodulation data at low temperature may be fitted according to a triple exponential function, as shown in Fig. 4a. However, using the same number of free parameters, the

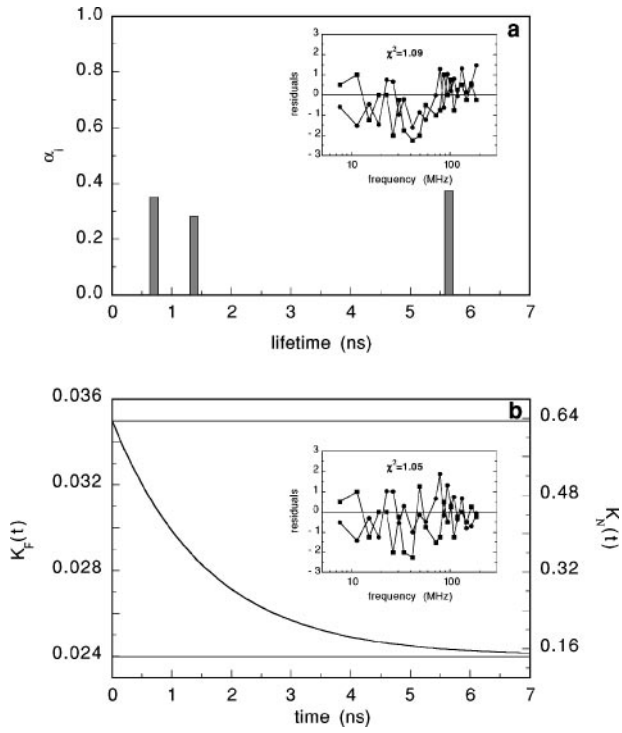

Fig. 4. Fluorescence decay parameters (see the legend of Fig. 1 for details) for staphylococcal nuclease in glycerol at −40°C. Panel a: triple exponential decay function parameters. Panel b (single relaxation function): $K_F^0 = 0.035 \pm 0.004$ ns^{-1}; $K_F^\infty = 0.024 \pm 0.003$ ns^{-1}; $K_N^0 = 0.63 \pm 0.02$ ns^{-1}; $K_N^\infty = 0.15 \pm 0.02$ ns^{-1}; $\tau_R = 1.59 \pm 0.05$ ns).

fluorescence decay may be alternatively interpreted in terms of a simple relaxation process (i.e. $\tau_F = \tau_N$), occurring in about 1.6 ns (Fig. 4b). It is worth mentioning that this value indicates a good correspondence with the relaxation time of 1.4 ns found with the traditional TRES methodology [34].

An excellent agreement with the literature has been also obtained in the case of RNAase T1. Previous measurements have been interpreted with a single exponential decay, characterized by an average lifetime of ≈3.9 ns [35,36]. In Fig. 5a we have reported the parameters obtained with a triple exponential decay law, which in fact displays a predominant component centered at 4 ns. Recently, it has been shown that the spectral relaxation of RNAase T1 also occurs with a simple exponential function ($\tau_R \approx 700$ ps) at 20°C [1]. In order to test whether it is possible to obtain the same result directly from the protein dynamic fluorescence, we fitted phase and demodulation data of RNAase T1 according to Eq. (10). The results, shown in Fig. 5b, demonstrate that the relaxation process may be characterized by a single relaxation time

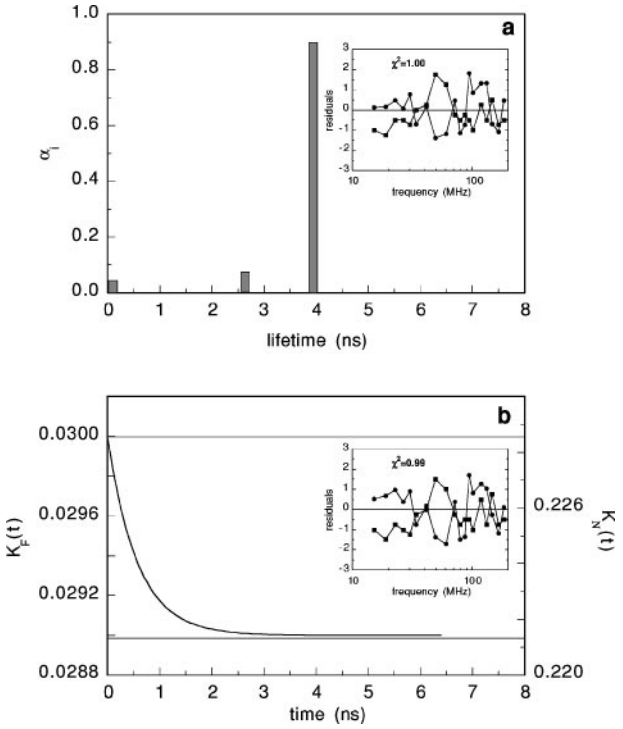

Fig. 5. Fluorescence decay parameters (see the legend of Fig. 1 for details) for RNAase-T1 in sodium acetate buffer (100 mM, pH 5.5) at 8°C. Panel a: triple exponential decay function parameters. Panel b (single relaxation function): $K_F^0 = 0.030 \pm 0.004$ ns^{-1}; $K_F^\infty = 0.029 \pm 0.003$ ns^{-1}; $K_N^0 = 0.23 \pm 0.02$ ns^{-1}; $K_N^\infty = 0.22 \pm 0.02$ ns^{-1}; $\tau_R = 0.57 \pm 0.03$ ns).

($\tau_F = \tau_N = 0.57$ ns), which is indeed very close to the value obtained using the traditional TRES methodology [1].

Among the other parameters which characterize the fitting function described by Eq. (10), the time dependence of K_F also correlate fairly well to the result of TRES measurements. For example, the time change of K_F is much smaller for RNAase T1 (Fig. 5b) than for staphylococcal nuclease (Fig. 4b), paralleling their spectral relaxation, which is known to be ≈44 cm^{-1} [1] and ≈600 cm^{-1} [34], respectively.

This coincidence also suggests that $K_F(t)$ is strictly correlated to the structural properties of the environment surrounding the tryptophanyl residue in the two proteins. In RNAase T1 Trp 59 is quite immobilized [37] and located in a rather hydrophobic pocket of the protein matrix, mainly consisting of apolar residues [38]. Thus, in buffer, at 20°C, the protein displays a very blue-shifted (≈325 nm) fluorescence spectrum [35]. On the other hand, several groups surrounding the single tryptophan of staphylococcal nuclease (Trp-140) are polar and display a high degree of segmental mobility [34], suggesting that at room temperature the fluorescence emission is due to fully relaxed states. This explains why the effect of relaxation on tryptophan fluorescence in the two proteins was observed under very different physico-chemical conditions, i.e. a much higher viscosity and low temperature in the case of staphylococcal nuclease.

Though a single relaxation process was sufficient to fit the data of both RNAase T1 and staphylococcal nuclease, this approach might not be valid for other proteins. In fact, due to the large set of different movements characterizing the protein matrix around the fluorophore, the relaxation process might be more complex, requiring more relaxation times. This hypothesis has been confirmed in the case of at least two proteins, namely melittin and HSA.

Melittin is a small protein of 26 aminoacids that is known to exist in an unfolded monomeric form in water. Under this condition the fluorescence emission of its single tryptophan residue is in fact red-shifted (≈350 nm) and does not show any dependence on the excitation wavelength [30]. On the other hand, the formation of a folded tetrameric structure has been observed upon increasing the ionic strength of the solution. In this oligomeric form the fluorescence emission is shifted to shorter wavelengths and displays a relevant red-edge effect already at 20–25°C [30]. Furthermore, time-resolved spectroscopy measurements revealed that the spectral shift during the excited state lifetime is strongly temperature dependent [39]. These features have been ascribed to dipolar structural relaxation of the tryptophanyl environment, characterized by relaxation times in the nanosecond range. A relevant dependence of the emission decay on the excitation wavelength was also observed for monomeric melittin in methanol [7]. In this case a double exponential function was used to represent the time-dependent shift of the emission spectrum [1,8].

We have measured the fluorescence dynamics of tetrameric folded melittin in order to recover information on the dipolar relaxation process directly from the emission decay. In particular, phase and demodulation data were fitted according to Eq. (10) with both $\tau_F = \tau_N$ and $\tau_F \neq \tau_N$. In the first case the same chi-squared value of a traditional triple-exponential fit was obtained (≈1.2), yielding weighted residuals which were not distributed according to a gaussian statistics as revealde by the Smirnov-Kolmogorov test [40]. Better residuals patterns and significantly lower chi-squared values were instead obtained with a double relaxation fit, in which $K_F(t)$ and $K_N(t)$ have an independent time-course (Fig. 6b). Indeed the relaxation time associated to $K_F(t)$, τ_F, is ≈5 times larger than τ_N, suggesting that the relaxation process is probably rather complex and consists of a hierarchy of different processes. Similar results were also obtained for folded

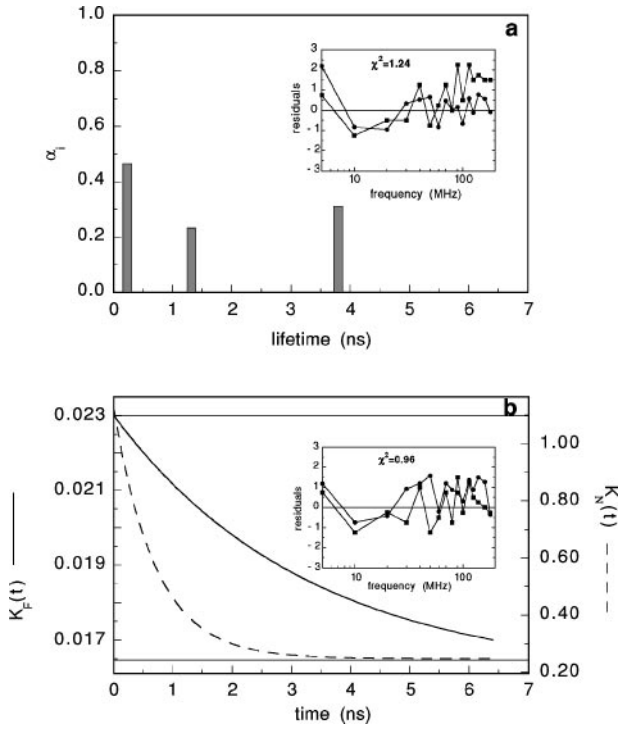

Fig. 6. Fluorescence decay parameters (see the legend of Fig. 1 for details) for tetrameric melittin (in Tris HCl, pH 7.5, 0.2 M NaCl) at 15°C. Panel a: triple exponential decay function parameters. Panel b (double relaxation function, i.e. $\tau_F \neq \tau_N$: $K_F^0 = 0.023 \pm 0.003$ ns^{-1}; $K_F^\infty = 0.016 \pm 0.003$ ns^{-1}; $K_N^0 = 1.12 \pm 0.09$ ns^{-1}; $K_N^\infty = 0.25 \pm 0.03$ ns^{-1}; $\tau_F = 3.28 \pm 0.06$ ns; $\tau_N = 0.71 \pm 0.05$ ns).

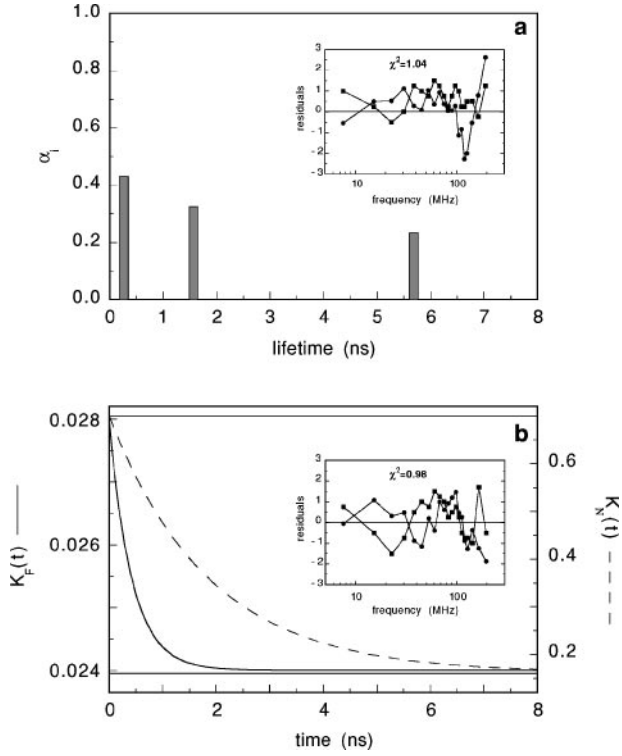

Fig. 7. Fluorescence decay parameters (see the legend of Fig. 1 for details) for HSA (in K-phosphate buffer, pH 6.0, 50 mM) at 20°C. Panel a: triple exponential decay function parameters. Panel b (double relaxation function, i.e. $\tau_F \neq \tau_N$: $K_F^0 = 0.028 \pm 0.002$ ns^{-1}; $K_F^\infty = 0.024 \pm 0.002$ ns^{-1}; $K_N^0 = 0.70 \pm 0.03$ ns^{-1}; $K_N^\infty = 0.16 \pm 0.02$ ns^{-1}; $\tau_F = 0.42 \pm 0.02$ ns; $\tau_N = 1.86 \pm 0.08$ ns.

melittin in ethanol (data not shown), confirming the occurrence of relaxation also in the folded monomeric protein, as recently reported by red-edge measurements in the time domain [7].

This heterogeneity is not a unique feature of the melittin molecule. For example, Buzàdy and coworkers [41] have recently demonstrated that also human serum albumin displays a complex red-shift decay of the time-resolved fluorescence spectrum. In particular they have found that dielectric relaxation of HSA in buffer, at ≈20°C, occurs according to a double relaxation process, characterized by both a fast (≈0.5 ns) and a slow (≈5 ns) component [41]. We have also studied the excited state dynamics of HSA using the phase and demodulation technique, fitting the data with the new approach. The results, reported in Fig. 7, point out to the presence of at least two relaxation times (≈0.3 and ≈4 ns), in close agreement with those previously found [41]. The presence of such a complex dynamics in the case of HSA has been ascribed to the different extension and frequency of the local segmental movements of the tryptophan environment [41]. As a borderline case, the possibility that a hierarchy of different substates could induce a continuous distribution of relaxation times has been also suggested [41], but not yet demonstrated since more accurate measurements are probably required. Our results are in line with this hypothesis since a fit of the protein dynamics in terms of a unique relaxation process yielded a much higher chi-squared value (≈1.8). Furthermore, with respect to the other proteins that we examined, HSA exhibits the largest difference between the radiative and non-radiative processes (more than on order of magnitude), suggesting that the events affecting the tryptophan excited state are characterized by quite different time scales.

Extension of the Relaxation Decay Model to Other Single Tryptophan-Containing Proteins

All the examples just discussed dealt with proteins displaying spectral relaxation in the nanosecond time range, as revealed by the traditional TRES methodology. In no case a single fluorescence lifetime characterized their

emission decay and this finding was previously ascribed to the presence of multiple conformational substates. On the other hand, we have shown how this dynamic fluorescence heterogeneity may be alternatively explained introducing the dipolar relaxation process directly in the decay function.

In this section we want to extend this new approach to the case of two single tryptophan-containing enzymes, namely HSOD and PFK. Despite in these two cases the presence of dipolar relaxation effects has not yet proved, we have recently shown that it is possible to fit the fluorescence dynamics of both PFK and HSOD in terms of a time-dependent emission rate function [13]. In PFK, Trp179 is not accessible to water molecules and its multiple exponential decay was previously attributed to distinct conformational substates characterizing the tryptophan microenvironment [42]. As shown in Fig. 8a and b, no qualitative distinction can be made between a multiple exponential decay function and a single relaxation model (no improvements were obtained using a double relaxation process). A very small change in the K_F value was obtained (Fig. 8b), suggesting that most of the effect is due to the non-radiative component (K_N) and providing a reasonable explanation for the absence of negative amplitudes in the longer lifetime range.

The dipolar relaxation process in PFK has been also studied by increasing the solvent viscosity but no relevant effect was observed in the presence of glycerol (Fig. 8c). This finding may be indeed explained on the basis of the enzyme tridimensional structure, considering the reduced solvent accessibility to the environment of Trp179.

In the case of HSOD the tryptophan residue is instead located on the external protein surface and displays a subnanosecond segmental mobility [14] in a quite restricted (≈15–20 deg) cone semi-angle [43]. The emission decay is complex and in fact one continuous distribution of lifetimes centered around 2.25 ns was previously used to fit the data [14]. The results of more recent experiments are reported in Fig. 9a and b and demonstrate that dipolar relaxation could also explain the protein fluorescence heterogeneity. At variance with PKF, a much stronger effect of glycerol was observed on the fluorescence dynamics of HSOD (Fig. 9c). In fact a double relaxation model was required to fit the data yielding very different values for τ_N and τ_F. Another opposite feature that distinguishes the two proteins' behavior is the different extent of the radiative rate change, $\Delta K_F = K_F^0 - K_F^\infty$ (cfr. Figs. 8 and 9), especially in the presence of glycerol. Despite a more detailed experimental analysis is required to explain quantitatively this result, it is clear that the tryptophan microenvironment plays a fundamental role in the dipolar relaxation process. In particular, the local dielectric constant (i.e. the local polarity) and the relative mobility of the tryptophan residue with respect to the surrounding groups are expected to influence dramatically the spectral relaxation. In this regard, we have compared the temporal spectral shift, $\Delta\lambda$, (when available from the literature) to the radiative rate change, ΔK_F, that we have obtained using Eq. (10). The result, reported in Fig. 10, demonstrates that indeed a correlation exists between the two parameters, thus providing further evidence that our new model is consistent with the time-resolved spectra obtained in the past in the same experimental condition.

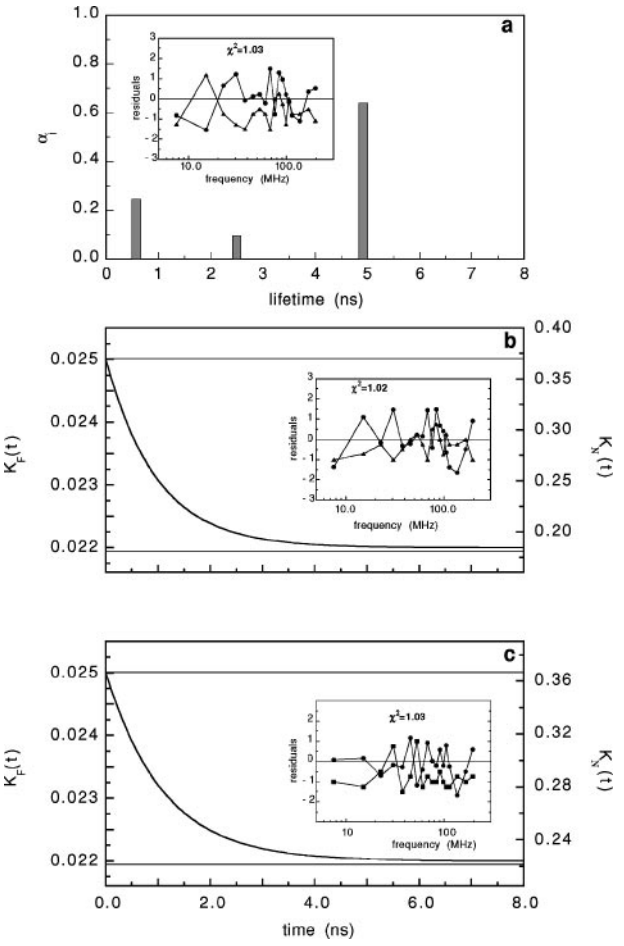

Fig. 8. Fluorescence decay parameters (see the legend of Fig. 1 for details) for PFK at 20°C. Panel a: triple exponential decay function parameters. Panel b (single relaxation function): $K_F^0 = 0.025 \pm 0.004$ ns^{-1}; $K_F^\infty = 0.022 \pm 0.002$ ns^{-1}; $K_N^0 = 0.37 \pm 0.05$ ns^{-1}; $K_N^\infty = 0.18 \pm 0.02$ ns^{-1}; $\tau_R = 0.97 \pm 0.07$ ns. Panel c: PFK in glycerol (single relaxation function): $K_F^0 = 0.025 \pm 0.004$ ns^{-1}; $K_F^\infty = 0.022 \pm 0.002$ ns^{-1}; $K_N^0 = 0.37 \pm 0.02$ ns^{-1}; $K_N^\infty = 0.22 \pm 0.02$ ns^{-1}; $\tau_R = 1.10 \pm 0.07$ ns.

In conclusion we have reported several examples of single probes in viscous media as well as in different

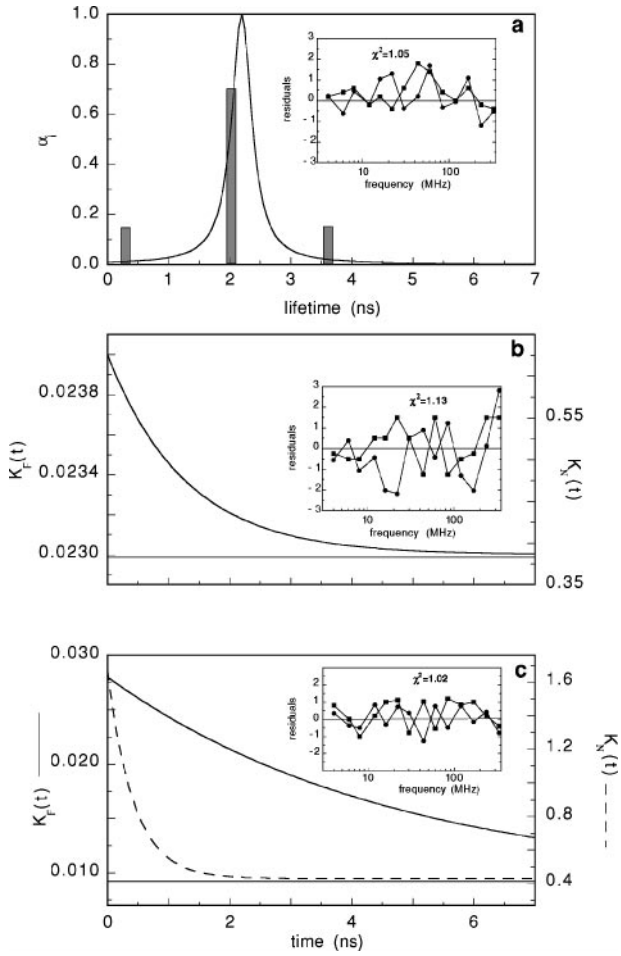

Fig. 9. Fluorescence decay parameters (see the legend of Fig. 1 for details) for HSOD at 20°C. Panel a: triple exponential decay function parameters. For comparison the lorentzian distribution previously obtained [14] has been also reported. Panel b (single relaxation function): $K_F^0 = 0.025 \pm 0.004$ ns^{-1}; $K_F^\infty = 0.024 \pm 0.002$ ns^{-1}; $K_N^0 = 0.65 \pm 0.07$ ns^{-1}; $K_N^\infty = 0.40 \pm 0.02$ ns^{-1}; $\tau_R = 0.86 \pm 0.06$ ns. Panel c: HSOD in glycerol (double relaxation function): $K_F^0 = 0.028 \pm 0.005$ ns^{-1}; $K_F^\infty = 0.009 \pm 0.003$ ns^{-1}; $K_N^0 = 1.65 \pm 0.08$ ns^{-1}; $K_N^\infty = 0.43 \pm 0.02$ ns^{-1}; $\tau_F = 4.66 \pm 0.08$ ns; $\tau_N = 0.33 \pm 0.02$ ns.

proteins whose dipolar relaxation has been evaluated directly from the fluorescence emission decay. With respect to the TRES methodology the new approach may offer the following advantages. i) The relaxation time can be directly obtained from the fluorescence decay; ii) the two contributions of the radiative and non-radiative decay rates can be resolved, allowing to detect dipolar relaxation effects also when the temporal spectral shift, $\Delta\lambda$, is very small, due to the peculiar physico-chemical characteristic of the tryptophan environment; iii) it provides an alternative explanation for the complex emission decays observed in single tryptophan-containing proteins.

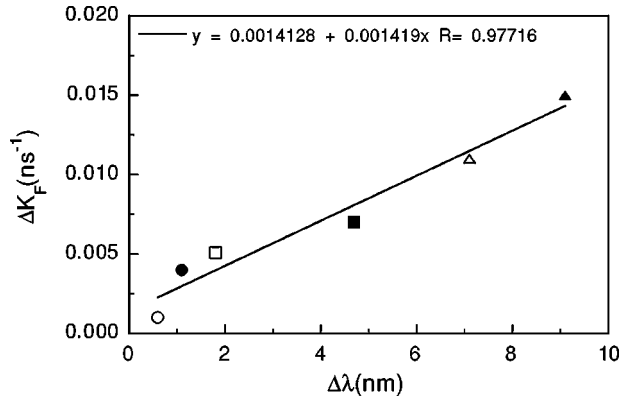

Fig. 10. Linear correlation between the radiative rate change, ΔK_F, and the spectral relaxation shift, $\Delta\lambda$ (where λ correspond to the spectral center of mass). Symbols correspond to the following samples: RNAase-T1 in buffer (empty circle); albumin in buffer (filled circle); staphylococcal nuclease in buffer (empty square); melittin in buffer (filled square); staphylococcal nuclease in glycerol at -40°C (empty triangle); indole in propylene glycol (filled triangle).

This last result might have critical consequences in the interpretation of the dynamic fluorescence data. In fact, excited state interactions that characterize the tryptophan photo-physics [24,44] are local processes. In particular, dielectric relaxation involves a restricted area around the tryptophan residue and it is not necessarily correlated to the much larger protein conformational changes generally invoked to justify a multiple exponential and/or a continuos distribution function for data analysis.

ACKNOWLEDGMENTS

This study was supported in part by grants from Ministry of Education (MIUR-COFIN 2001, 2002), Italy.

REFERENCES

1. J. R. Lakowicz (2000). *Principles of Fluorescence Spectroscopy*, 2nd ed., Kluwer Academic, New York.
2. J. B. A. Ross, W. R. Laws, K. W. Rousslang, and H. R. Wyssbrod (1992). in J. R. Lakowicz (Ed.), *Topics in Fluorescence Spectroscopy*, Vol. 3, Plenum Press, New York, chap. 1.
3. C. Eggeling, S. Berger, L. Brand, J. R. Fries, J. Schaffer, A. Volkmer, and C. A. Seidel, (2001). Data registration and selective single-molecule analysis using multi-parameter fluorescence detection. *J. Biotechnol.* **86**, 163–180.
4. L. S. Slater and P. R. Callis (1995). Molecular orbital theory of the ^{1}La ans ^{1}Lb states of indole. 2. An ab initio study. *J. Phys. Chem.* **99**, 8572–8581.
5. A. P. Demchenko (1986). *Ultraviolet Spectroscopy of Proteins*, Springer-Verlag, Berlin.
6. M. Vincent, J. Gallay, and A. P. Demchenko (1997). Dipolar relaxation around indole as evidenced by fluorescence lifetime

distributions and time-dependence spectral shifts *J. Fluoresc.* **7**, 107S–110S.
7. A. S. Ladokhin (1999). Red-edge excitation study of non-exponential fluorescence decay of indole in solution and in a protein *J. Fluorescesc.* **9**, 1–10.
8. J. R. Lakowicz (2000). On spectral relaxation in proteins. *Photochem. Photobiol.* **72**, 421–437.
9. B. De Foresta, J. Gallay, J. Sopkova, P. Champeil, and M. Vincent (1999). Tryptophan octyl ester in detergent micelles of dodecylmaltoside: Fluorescence properties and quenching by brominated detergent analogs. *Biophys. J.* **77**, 3071–3084.
10. H. A. Garda, A. M. Bernasconi, R. R. Brenner, F. Aguilar, M. A. Soto, and C. P. Sotomayor (1997). Effect of polyunsaturated fatty acid deficiency on dipole relaxation in the membrane interface of rat liver microsomes. *Biochim. Biophys. Acta* **1323**, 97–104.
11. L. A. Bagatolli, T. Parasassi, G. D. Fidelio, and E. Gratton (1999). A model for the interaction of 6-lauroyl-2-(*N*,*N*-dimethylamino)naphthalene with lipid environments: Implications for spectral properties. *Photochem. Photobiol.* **4**, 557–564.
12. S. S. Antollini, M. A. Soto, I. Bonini de Romanelli, C. Gutierrez-Merino, P. Sotomayor, and F. J. Barrantes (1996). Physical state of bulk and protein-associated lipid in nicotinic acetylcholine receptor-rich membrane studied by laurdan generalized polarization and fluorescence energy transfer. *Biophys. J.* **70**, 1275–1284.
13. G. Mei, A. Di Venere, F. De Matteis, and N. Rosato (2003). The recovery of dipolar relaxation times from fluorescence decays as a tool to probe local dynamics in single tryptophan proteins. *Archives Biochem. Biophys.* **417**, 159–164.
14. G. Mei, N. Rosato, N. Silva, R. Rusch, E. Gratton, I. Savini, and A. Finazzi Agrò (1992). Denaturation of human Cu/Zn superoxide dismutase by guanidine hydrochloride: A dynamic fluorescence study. *Biochemistry* **31**, 7224–7230.
15. E. Gratton, and M. Limkeman (1983). A continuously variable frequency cross-correlation phase fluorometer with picosecond resolution. *Biophys. J.* **44**, 315–325.
16. G. Mei, A. Di Venere, F. De Matteis, A. Lenzi, and N. Rosato (2001). Asymmetrical distribution of intrinsic fluorescence lifetimes in proteins. *J. Fluorescence* **11**, 319–333.
17. J. R. Alcala, E. Gratton, and F. G. Prendergast (1987). Fluorescence lifetime distributions in proteins. *Biophys. J.* **51**, 597–604.
18. J. R. Lakowicz, H. Cherek, I. Gryczynski, N. Joshi, and M. L. Johnson (1987). Analysis of fluorescence decay kinetics measured in the frequency domain using distributions of decay times. *Biophys. Chem.* **28**, 35–50.
19. Ware, W. R. (1992). in V. Ramamurthy (Ed.), *Photochemistry in organized and costrained media*, VCA Publisher, New York, chap. 13.
20. A. G. Szabo, and D. M. Rayner (1980). Fluorescence decay of tryptophan conformers in aqueous solution. *J. Am. Chem. Soc.* **102**, 554–563.
21. J. W. Petrich, M. C. Chang, D. B. McDonald, and G. R. Fleming (1983). On the origin of nonexponential fluorescence decay in tryptophan and its derivatives. *J. Am. Chem. Soc.* **105**, 3824–3836.
22. R. F. Chen, J. R. Knutson, H. Ziffer, and D. Porter (1991). Fluorescence of tryptophan dipeptides: Correlations with the rotamer model. *Biochemistry* **30**, 5184–5195.
23. B. Liu, R. K. Yhalji, P. D. adams, F. R. Fronczek, M. L. McLaughlin, and M. D. Barkley (2002). Fluorescence of cis-1-Amin-2-(3-indolyl)cyclohexane-1-carboxylic acid: A single tryptophan χ_1 rotamer model. *J. Am. Chem. Soc.* **124**, 13329–13338.
24. M. R. Eftink, Y. Jia, D. Hu, and C. A. Ghiron (1995). Fluorescence studies with tryptophan analogs: excited state interactions involving the side chain amino group. *J. Phys. Chem.* **99**, 5713–5723.
25. J. R. Lakowicz, and H. C. Cherek (1980). Dipolar relaxation in proteins on the nanosecond timescale observed by wavelength-resolved phase fluorometry of tryptophan fluorescence. *J. Biol. Chem.* **255**, 831–834.
26. A. P. Demchenko, and A. S. Ladokhin (1988). Red-edge-excitation fluorescence spectroscopy of indole and tryptophan. *Eur. Biophys. J.* **15**, 369–379.
27. J. R. Lakowicz, H. Szmacinski, and I. Gryczynski (1988). Picosecond resolution of indole anisotropy decays and spectral relaxation by 2 GHz frequency-domain fluorometry. *Photochem. Photobiol.* **47**, 31–41.
28. D. Toptygin and L. Brand (2000). Spectrally- and time-resolved fluorescence emission of indole during solvent relaxation: A quantitative model. *Chem. Phys. Lett.* **322**, 496–502.
29. E. J. P. Malar and K. Jug (1984). Structures and properties of excited states of benzene and some monosubstituted benzenes. *J. Phys. Chem.* **88**, 3508–3516.
30. A. P. Demchenko (1988). Red-edge-excitation fluorescence spectroscopy of single-tryptophan proteins. *Eur. Biophys. J.* **16**, 121–129.
31. P. R. Callis (1997). ^{1}La and ^{1}Lb transitions of tryptophan: Applications of theory and experimental observations to fluorescence of proteins. *Methods Enzymol.* **278**, 113–150.
32. M. R. Eftink, I. Gryczynski, W. Wiczk, G. Laczko, and J. R. Lakowicz (1991). Effects of temperature on the fluorescence intensity and anisotropy decays of staphylococcal nuclease and the less stable nuclease-conA-SG28 mutant. *Biochemistry* **30**, 8945–8653.
33. A. J. W. G. Visser, J. van Engelen, N. V. Visser, A. van Hoek, R. Hilhorst, and R. B. Freedman (1994). Fluorescence dynamics of staphylococcal nuclease in aqueous solution and reversed micelles. *Biochim. Biophys. Acta* **1204**, 225–234.
34. A. P. Demchenko, I. Gryczynsky, Z. Gryczynsky, W. Wiczk, H. Malak, and M. Fishman (1993). Intramolecular dynamics in the environment of the single tryptophan residue in staphylococcal nuclease. *Biophys. Chem.* **48**, 39–48.
35. M. Eftink and C. A. Ghiron (1987). Frequency domain measurements of the fluorescence lifetime of ribonuclease T1. *Biophys. J.* **52**, 467–473.
36. I. Gryczynski, M. Eftink, and J. R. Lakowicz (1988). Conformation heterogeneity in proteins as an origin of heterogeneous fluorescence decays, illustrated by native and denatured ribonuclease T1. *Biochim. Biophys. Acta* **954**, 244–252.
37. J. R. Lakowicz, B. P. Maliwal, H. Cherek, and A. Balter (1983). Rotational freedom of tryptophan residues in proteins and peptides. *Biochemistry* **22**, 1741–1752.
38. U. Heinemann and W. Saenger (1982). Specific protein-nucleic acid recognition in ribonuclease T1-2′-guanylic acid complex: An X-ray study. *Nature* **299**, 27–31.
39. A. P. Demchenko and A. S. Ladokhin (1988). Temperature-dependent shift of fluorescence spectra without conformational changes in protein; studies of dipole relaxation in the melittin molecule. *Biochim. Biophys. Acta* **955**, 352–360.
40. M. Fisz (1963). *Probability Theory and Mathematical Statistics*, Wiley, New York, chap. 12.
41. A. Buzády, J. Erostyák, and B. Somogyi (2000). Phase-fluorimetry study on dielectric relaxation of human serum albumin. *Biophys. Chem.* **88**, 153–163.
42. S. J. Kim, F. N. Chowdhury, W. Stryjewski, E. S. Younathan, P. S. Russo, and M. D. Barkley (1993). Time-resolved fluorescence of the single tryptophan of Bacillus stearothermophilus phosphofructokinase. *Biophys. J.* **65**, 215–226.
43. N. Silva, E. Gratton, G. Mei, N. Rosato, R. Rusch, and A. Finazzi Agro' (1993). Molten globule monomers in human superoxide dismutase. *Biophys. Chem.* **48**, 171–182.
44. Y. Chen and M. D. Barkley (1998). Toward understanding tryptophan fluorescence in proteins. *Biochemistry* **37**, 9976–9982.